Microsc. Microanal. 11, 300–312, 2005
DOI: 10.1017/S143192760505021X

Microscopy AND Microanalysis

Reproductive Cytotoxicity Is Predicted by Magnetic Resonance Microscopy and Confirmed by Ubiquitin–Proteasome Immunohistochemistry in a Theophylline-Induced Model of Rat Testicular and Epididymal Toxicity

M.W. Tengowski,[1,*] P. Sutovsky,[2] L.W. Hedlund,[3] D.J. Guyot,[1] J.E. Burkhardt,[1] W.E. Thompson,[4] M. Sutovsky,[2] and G.A. Johnson[3]

[1]*Safety Sciences Groton, Pfizer Global Research & Development, Groton, CT 06340, USA*
[2]*Departments of Animal Science and Obstetrics & Gynecology, University of Missouri-Columbia, Columbia, MO 65211, USA*
[3]*Center for In Vivo Microscopy, Duke University, Durham, NC 27710, USA*
[4]*Cooperative Reproductive Science Research Center, Morehouse School of Medicine, Atlanta, GA 30310, USA*

Abstract: This study investigated the testicular changes in the rat induced by the nonspecific phosphodiesterase inhibitor, theophylline using magnetic resonance microscopy (MRM) and ubiquitin immunostaining techniques. *In vivo* T1- and T2-weighted images were acquired at 2 T under anesthesia. Increased signal observed in the theophylline-treated rats suggests that leakage of MRM contrast was occurring. *In vivo* MRM results indicate that day 16 testis displayed an increased T1-weighted water signal in the area of the seminiferous tubule that decreased by day 32. These findings were validated by histopathology, suggesting that *in vivo* MRM has the sensitivity to predict changes in testis and epididymal tissues. The participation of the ubiquitin system was investigated, using probes for various markers of the ubiquitin-proteasome pathway. MRM can be used to detect subtle changes in the vascular perfusion of organ systems, and the up-regulation/mobilization of ubiquitin-proteasome pathway may be one of the mechanisms used in theophylline-treated epididymis to remove damaged cells before storage in the cauda epididymis. The combined use of *in vivo* MRM and subsequent tissue or seminal analysis for the presence of ubiquitin in longitudinal studies may become an important biomarker for assessing testis toxicities drug studies.

Key words: magnetic resonance imaging, microscopy, reproduction, toxicology, theophylline, rat, testis, epididymis, ubiquitin, proteasome, Arylsulfatase A

Introduction

Theophylline (1,3-dimethylxanthine) was first isolated from tea and chocolate, and has been used clinically to treat asthma and emphysema by relaxing the bronchiole smooth muscles. The finding that feeding of methylxanthines to male rats produces impaired spermatogenesis and testicular atrophy at the gross and histologic level has been well studied. The male rat gonad appears to be especially sensitive to the effects of this drug class (Weinberger et al., 1978). The subtle sensitivity of the testis to oral theophylline administration may prove useful as a test compound for methods development. We used theophylline mixed in the feed to induce toxicity in an effort to assess the feasibility and sensitivity of magnetic resonance microscopy (MRM) in longitudinal safety toxicology studies. The image data collected with this noninvasive imaging technique were confirmed with conventional histopathology and immunohistochemical survey of the ubiquitin–proteasome pathway for protein degradation.

The use of magnetic resonance imaging (MRI), first suggested by Lauterbur (1973) is now routine in clinical medicine (Wehrli et al., 1988). The MRI technique relies heavily on the spin physics of hydrogen (Callaghan, 1993). The spin characteristics of the hydrogen proton are different with respect to chemical composition. Taken broadly, most of the body's protons are either water (H_2O), protein, or fat ($-CH_2-$ or $-CH_3$ groups). When a biological sample is placed in a high magnetic field, the protons align with the field and begin to precess at a very explicit frequency (the Larmor frequency) that depends on the field and the chemical state of the protons. The precessing protons can be

Received July 3, 2003; accepted August 25, 2004.
*Corresponding author. E-mail: mark_w_tengowski@groton.pfizer.com

excited and induced to yield a radio frequency signal by application of a series of radio frequency pulses at the Larmor frequency. The location of collections of the excited protons is encoded through the use of magnetic field gradients that spatially encode signals based on different frequencies. The protons subsequently relax to their initial condition and the entire process can be repeated. The protons relax at different rates depending on their local environment. Detecting where and how these protons relax can be used as a major source of image contrast. The water relaxation can be enhanced through the use of contrast agents such as gadolinium-containing compounds. The technique is considered noninvasive because it does not rely on ionizing radiation (i.e., radiographs, CT scanners).

Because MRI is a volumetric imaging technique, resolution can be most appropriately compared by considering the volume of the tissues elements (voxels) that generate the signal in each of the discrete picture elements (pixels). A typical body scan in a clinical MR system records signals from 10-mm-thick slices with voxel dimensions of $1 \times 1 \times 10$ mm, that is, voxel volume of 10 mm^3. Motion, a major limitation in the spatial resolution, can be controlled through the use of scan synchronous ventilation in which the anesthetized animal is mechanically ventilated in synchrony with the image acquisitions. With the combination of scan synchronous ventilation, operation at higher magnetic field, and the use of specialized radio frequency coils, it is possible to operate at much higher spatial resolution than is common in the clinical domain. The voxels for the *in vivo* animal studies reported here were $0.1 \times 0.1 \times 0.3$ mm (3×10^{-3} mm^3). The voxels in the *ex vivo* studies were $0.05 \times 0.05 \times 0.05$ mm (1.25×10^{-4} mm^3; that is, 80,000 times smaller than those of a typical clinical body scan). These increases in resolution do not come without cost. One of the trade-offs with MRM is the increase in overall scan time. This is a consideration for experimental design where daily throughput is a necessity.

The ubiquitin–proteasome pathway in the testis and epididymis is the major proteolytic system likely to be affected by reproductive toxicants. Ubiquitin is the cellular housekeeping peptide involved in the degradation of damaged and outlived proteins (for reviews, see Hershko, 1998; Pickart, 1998). The unconjugated ubiquitin molecule consists of 76 amino acids, with a molecular mass of 8.5 kDa. Ubiquitin binds to the other substrate proteins via its C-terminal, glycine residuum (G-76), forming an isopeptide bond with a lysine (K) residuum on the substrate protein. Similarly, ubiquitin molecules can bind to each other, forming ubiquitin chains of various lengths. All seven lysine residues in the ubiquitin molecule have been shown to be able to initiate such polyubiquitin chains. The most common signal for protein degradation is tetra-ubiquitination, that is, the formation of a four-ubiquitin chain on a substrate protein. This targets and docks the tetra-ubiquitinated substrate toward the proteasome, a multisubunit protease/proteolytic organelle common in most eukaryotic cells. Proteasomes degrade the target protein whereas the ubiquitin molecules of the docked polyubiquitin chain are released and used to regenerate the pool of monoubiquitin (Hochstrasser, 2002), but otherwise left intact and returned to the cytosol, where they become available again for ubiquitination of other proteins (Pickart, 1998). In contrast to tetra- or polyubiquitination-dependent proteasomal degradation, monoubiquitination is a consensus signal for the endocytosis of membrane receptors and possibly other proteins, after which such monoubiquitinated substrates may be degraded by a lysosome.

The apocrine secretion of ubiquitin by the epididymal epithelium was first suggested by Santamaria et al. (1993). Lippert et al. (1993) observed ubiquitin in human seminal plasma, but found no correlation with fertility or sperm quality. Sutovsky et al. (2001*b*) first observed that increased accumulation of ubiquitin on the surface of the defective mammalian spermatozoa correlated with poor sperm quality and infertility. Concomitant studies provided the initial evidence that ubiquitin was secreted by the epididymal epithelium as a monomer (Sutovsky et al., 2001*a*). These observations led Sutovsky to propose that a sperm quality control mechanism based on the secretion and binding of ubiquitin to defective spermatozoa, resides in the mammalian epididymis. This hypothesis was recently supported by the independent observations of ubiquitin secretion by the apical blebs in the rat epididymis (Hermo & Jacks, 2002).

We report here that changes in the male rat gonads induced by oral administration of theophylline present in the feed can be appreciated in the live animal as detected using MRM and confirmed with histology and an immunocytochemical survey of the resident testicular and epididymal ubiquitin–proteasome system. The pathophysiology of these findings is placed into context with the ubiquitin degradation pathway, and a new view of the role of the epididymis in clearing damaged sperm is discussed.

Materials and Methods

Animals, Treatment, and Experimental Design

All procedures and experimental protocols were reviewed and approved by the Animal Use and Care Committee at Groton Laboratories, and housed in facilities accredited by the Association for the Assessment and Accreditation of Laboratory Animal Care. Groups of male Crl:CD® (SD)BR VAF/Plus® rats were housed singly and given theophylline daily at 0 (2 animals per group) or 8000 ppm (3 animals per group) in feed for 8, 16, 24, or 32 consecutive days (Sigma Chemical Co., St. Louis, MO, lot number 68H06010). All rats were observed at least two times daily in their cages for signs of toxicity and for any changes in appearance or behavior. Prestudy body weights were collected at 1 day prior to the initiation of dosing. Thereafter, body weights were determined weekly during the study period, and again

on the day of imaging. Food consumption was measured weekly during the study period. The start date of each group was coordinated to accommodate *in vivo* MRM on a given day. Animals on study were shipped via overnight carrier from Groton Laboratories to the Duke University Medical Center 2 days prior to imaging. Rats were fasted overnight prior to imaging. On a given imaging day, both 0- and 8000-ppm theophylline-fed animals were imaged. These animals were weighed, anesthetized, catheterized for constant-rate infusion of contrast agent (gadolinium-DTPA, Magnevist®, 5 μl/min, http://www.schering-diagnostics.de/phys/products/mri/magnevist.htm) and positioned for imaging by MRM. Left and right testes and epididymes were collected, weighed, and processed for microscopic examination. Testes were post-fixed in Bouin's fixative prior to trimming, dehydrating, embedding in paraffin, sectioning, and mounting on glass slides. Slides were used for staining with hematoxylin and eosin for histopathologic evaluation, and for immunofluorescence detection of the components of the ubiquitin–proteasome pathway.

In Vivo Magnetic Resonance Microscopy, 2T

Multislice spin-echo encoding was used for the T1 and T2 scans. T1 scan parameters were as follows: TR = 500 ms, TE = 13 ms, number of averages = 8, field of view = 25.6 mm, field of view in phase = 25.6 mm, 256 × 256 pixels in-plane. T2 scan parameters wereas follows: TR = 2000 ms, TE = 100 ms, number of averages = 4, field of view = 25.6 mm, field of view in phase = 25.6 mm, 256 × 256 pixels in-plane, 300 μm slice thickness, 15 slices.

Ubiquitin–Proteasome Immunohistochemistry and Dual TUNEL–Ubiquitin Assay

Paraffin tissue sections (4 μm) were cut, placed on microscopy slides, dewaxed by xylene, and rehydrated in a 100–70% ethanol series and water. Tissue autofluorescence was reduced by a 20-min treatment with citric acid buffer (pH 6.0) using a steamer. Nonspecific reactions were blocked by preincubation with 5% normal goat serum (NGS) in phosphate-buffered saline (PBS) containing 0.1% Triton X-100 (TX-100; Sigma). Blocking and antibody incubations were performed in the dark and high humidity on a shielded histological tray filled with a water-soaked tissue paper. Slides were overlaid and incubated for 2 h with either anti-ubiquitin antibody KM-691, raised against the whole molecule of recombinant human ubiquitin, or with antibody MC-034, raised against peptide containing the sequence of ubiquitin–ubiquitin isopeptide bonds. Whereas the former antibody recognizes many of the unconjugated monoubiquitin and some of the ubiquitinated substrates, the later antibody has high affinity to polyubiquitin chains. Both antibodies were purchased from Kamiya Biomedical Company, Seattle, Washington, and used at a dilution of

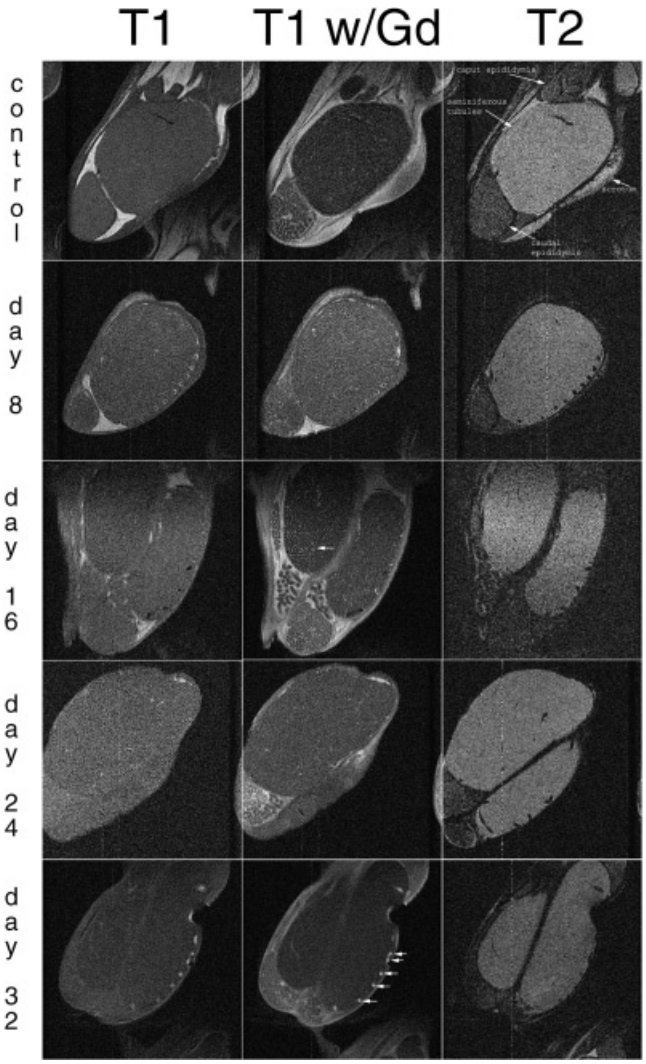

Figure 1. Composite magnetic resonance plate. Mid-sagittal scan slice from each sequence is represented. The presence of gadolinium increases the contrast in the T1-weighted series. A hyperintense pattern of the seminiferous tubules and cauda epididymis at day 16. Theophylline is the earliest sign of change appreciated by MR (white arrows). By day 32, the theophylline-treated testes are much smaller in sagittal section, plus the vascular pattern of the tunica (small white arrows) is more prominent, exacerbated by the presence of gadolinium in the vessel lumen. T2 tissue characteristics remain constant over the test period.

1/200. For dual labeling experiments, these antibodies were combined with rabbit polyclonal antibody against proteasomal core subunit β1i (Groettrup et al., 1996) or rabbit polyclonal antibody α/β recognizing proteasomal core subunits α5/α7, β1, β5, β5i, and β7subunit (Tanaka & Tsurumi, 1997), both purchased from Affinity Research Products, Ltd., Mammhead, United Kingdom (diluted 1/200) or a rabbit immune serum (diluted 1/100) raised by immunization of rabbits with the isolated 64-kDa bull sperm protein, and shown by MALDI-TOF microsequencing and recombi-

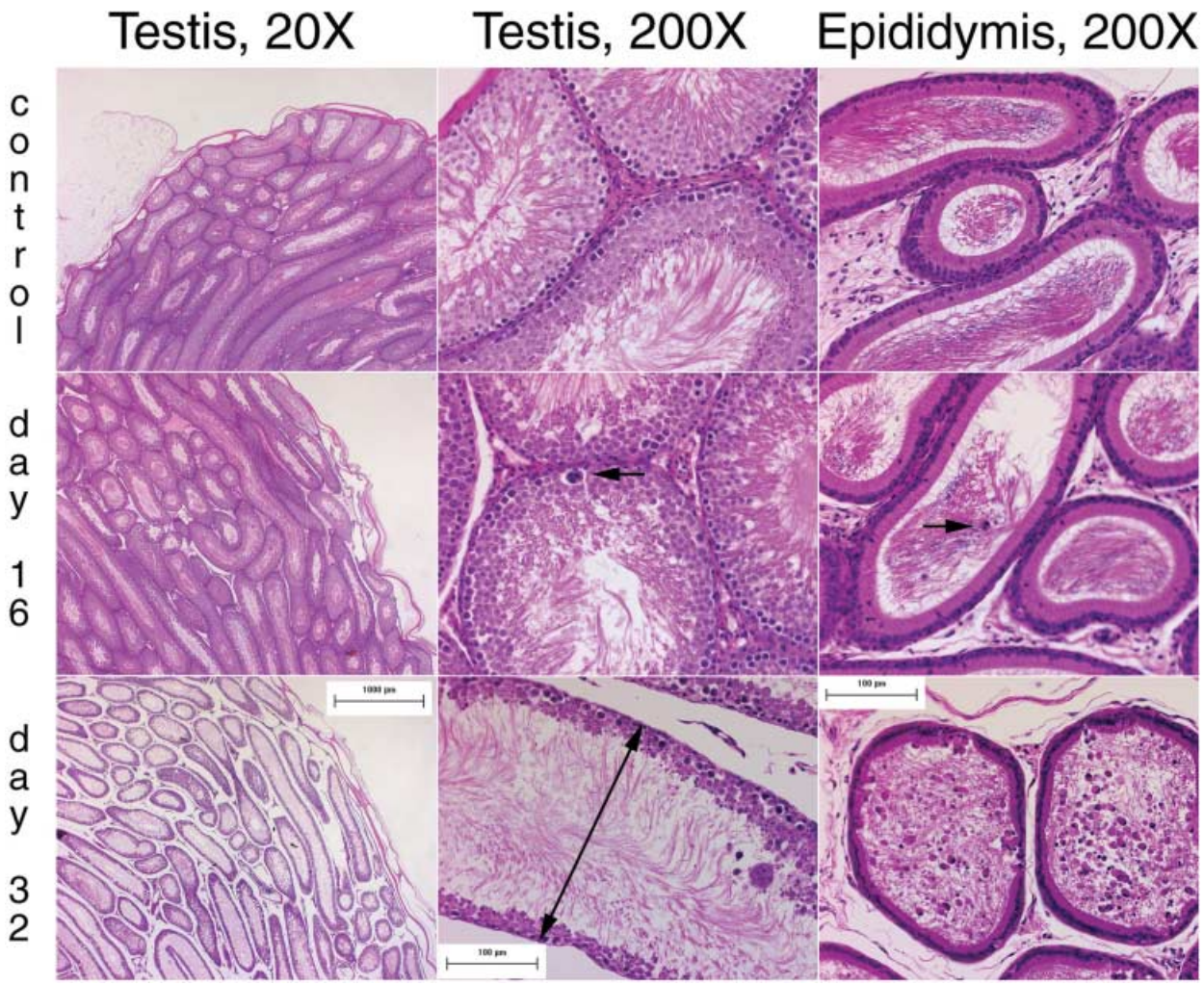

Figure 2. Histology plate of testis and epididymis tissues. Histological cross sections of the testis and epididymis chronicle the progression of the pathological findings. At day 16, testicular findings were limited to occasional multinucleate giant cells in the seminiferous tubules and abnormal content in the epididymis (black arrows). By day 32, there was degeneration and atrophy of the seminiferous epithelium with tubular dilatation (black arrow) and abnormal content within the epididymis lumen.

nant protein technology to recognize the sperm and epididymal deglycosylating enzyme, Arylsulfatase A (Thompson et al., 2002). After a vigorous washing, the slides were incubated with a combination of green fluorescent, FITC-conjugated goat anti-rabbit IgG and a red fluorescent, TRITC-conjugated goat anti-mouse IgM, both diluted to 1/80 in PBS with 1% NGS and 0.1% TX-100 and purchased from Zymed Inc., South San Francisco, California. For the dual, TUNEL-ubiquitin immunohistochemical assay, tissue sections were incubated with the green-fluorescent TUNEL solution (Roche Diagnostic Corp., Indianapolis, IN) for 1 h at 37°C in the dark and high humidity, then blocked and incubated with anti-ubiquitin KM-691 and a red-fluorescent anti-mouse IgM (Sutovsky et al., 2002). Following a wash in labeling solution, slides were overlaid with Vecta Shield mounting medium, covered with 22 × 88 mm microscopy coverslips, sealed with a transparent nail polish, and viewed in the Nikon Eclipse 800 epifluorescence microscope using appropriate filter sets and DIC optics. Images were acquired with a CoolSNAP CCD HQ camera (Roper Scientific, Tucson, AZ) and MetaMorph software (Universal Imaging Corp., Downington, PA), archived on recordable CDs, edited using Adobe Photoshop 5.5 (Adobe Systems, Mountain View, CA) and printed on a digital photo printer.

Statistics

Body weight, food consumption, and organ weights were analyzed statistically. Statistical analyses were performed separately each collection period, with each treated group

mean compared with the control group mean using a two-tailed Student's *t* test from the statistical package in MS Excel (version 97-SR2). A p value of 0.05 was used for significance.

Results

Overall Animal Health and Body Weights

All rats survived to the conclusion of the study. Clinical signs and observations related to theophylline treatment were limited to rough fur that was observed in most animals treated for 14 days or longer. One animal in the day-32 theophylline treatment group died during the induction phase of anesthesia, and MRM was not performed. There was a treatment and time-dependent reduction in terminal body weights in theophylline-treated animals compared to controls (0.85-, 0.72-, 0.60-, and 0.46*x* control after 8, 16, 24, and 32 days of treatment, respectively). This reflected both reduced weight gain and gradual weight loss over the course of the study, which was most pronounced during the first week of treatment. With the exception of control group 4, which lost 2.19 g within the week after shipment to Duke University, control rats gained an average 6.7 g during the first week on study. In contrast, theophylline-treated rats lost an average 6.5 g during the first week of treatment. This correlated with reduced food intake, which was observed in all theophylline-treated animals (average 0.42*x* control intake). Transportation to the MRM facility on day 24 of the study complicated evaluation of body weight and food intake. Food consumption for the week of shipment averaged 0.74 times that observed preshipment in both control and theophylline-treated rats. This resulted in reduced weight gains on days 8, 16, and 24 groups (0.4*x* average preshipment weight gains) and weight loss in the day-32 control group and all treated groups, with an average loss of 2.822 g (range 0.5–8.497 g).

Testis and Epididymis Weights

Control measures were not different on different study days ($p = 0.647$ for testes, $p = 0.801$ for epididymes) and were subsequently combined for statistical purposes. Testicular weights were normal in the 8-, 16-, and 24-day treatment groups, but reduced in the 32-day treatment group ($p < 0.001$). Epididymal weights were significantly reduced in all treatment groups ($p < 0.029$ for day 8, $p < 0.013$ for day 16, $p < 0.001$ for day 24, $p < 0.001$ for day 32).

In Vivo MRM at 2T

Positioning the rat for live animal imaging is a special consideration. To optimize the MRM signal, a special acrylic carrier was constructed to allow the scrotum to hang freely, with the RF coil positioned in close proximity. The scans were performed with a T1 spin echo without contrast agent, a T2 scan, and a final T1 scan with a constant rate infusion of contrast agent (Fig. 1). Control animals were screened every day with the selected experimental animals grouped by days-in-feed treatment. The day-8 theophylline group did not show any differences in testis images. The day-16 group, however, displayed a hyperintensity within the area of the seminiferous tubules, much different than that observed in the control images. An increased signal in the caudal epididymis was also observed in the contrast-agent-enhanced T1 images. By day 32, a decrease in the testis cross section in the sagittal plane was seen, with a decrease in blood flow through the tunica albiginea as indicated by the presence of signal in the vessels. Normally, blood flows out of the plane of image, and is perceived as the absence of signal (black holes in control vessel lumen).

Light Microscopic, Histological Findings

Right and left testes and epididymes were examined microscopically (Fig. 2). Slight to mild testicular degeneration, characterized by loss of spermatocytes, retention of spermatids, formation of variable numbers of multinucleated cells, and/or dilatation of seminiferous tubules, was present in all theophylline-treated animals euthanized on days 24 and 32; in 2 of 3 animals euthanized on day 16; and in 0 of 3 animals euthanized on day 8. In most animals the testicular degeneration was bilateral, although unilateral changes were observed in 1 animal evaluated on day 24 and in 1 animal evaluated on day 16. Although testicular changes were not

Figure 3. Monoubiquitin and Arylsulfatase A immunodetection. Epididymal secretion of the monomeric ubiquitin and Arylsulfatase A (AsA) screened using monoclonal antibody KM691 against recombinant human ubiquitin (red) and anti-AsA-serum (green) in control (**A**, **B**) and theophylline-treated rats (**C**–**F**). A basal level of ubiquitin cross-reactivity in the epididymis of control rat tissues (**A**, **B**). Note the accumulation of ubiquitin (red dots) in the cytoplasmic droplets present in the epididymal spermatozoa of both control (**B**) and treated rats (**C**). There is a strong accumulation of monoubiquitin on the epididymal epithelial lining, suggestive of increased secretion by the apical blebs seen in the treated rat tissues (**D**, **E**). **F:** Differential-interference contrast image of the apical blebs, displaying the characteristic large bulbous projections of the principal cells, through which secretory proteins are released into epididymal lumen. Diagram included to shows the respective patterns of ubiquitin chain formation recognized by antibodies KM691 (unconjugated and substrate-conjugated monoubiquitin) and MC034 (polyubiquitin chains).

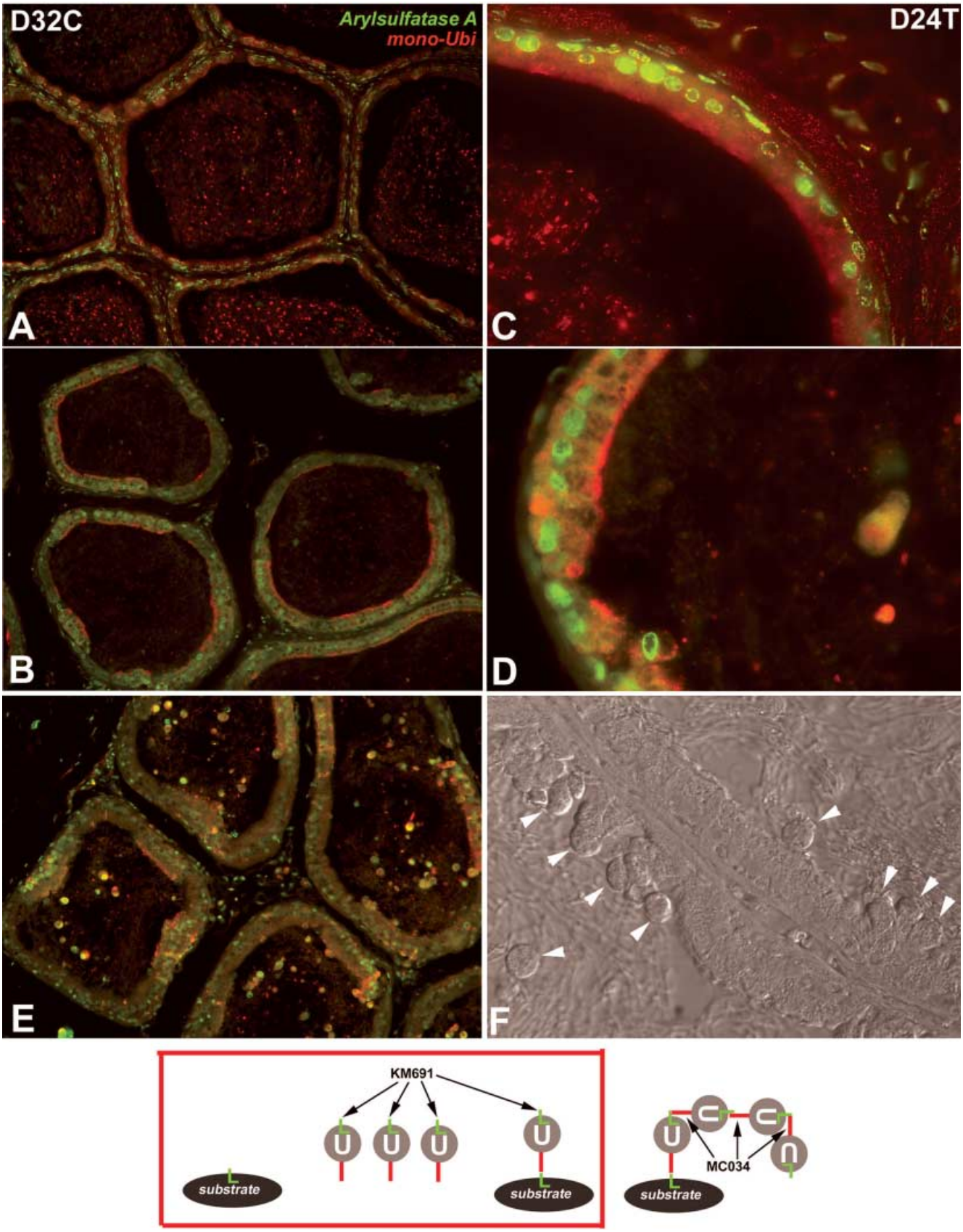

microscopically evident in rats treated with theophylline for only 8 days, abnormal epididymal content consisting of sloughed and degenerate spermatocytes or epididymal epithelial cells, epididymal apical blebs, and multinucleated cells were present in 2 of 3 animals evaluated on day 8 and in all animals treated for longer periods. In addition to abnormal content, degeneration of epididymal epithelium was observed in 1 of 3 animals on day 8, 0 of 3 animals on day 16, 2 of 3 animals on day 24, and 2 of 3 animals on day 32, the significance of which is uncertain.

Immunohistochemical Detection of the Components of the Ubiquitin–Proteasome Pathway in the Testis and Epididymis

Monomeric ubiquitin (monoubiquitin) and monoubiquitin moieties conjugated to substrate proteins during proteolytic degradation/endocytosis were detected using monoclonal antibody KM691 against recombinant human ubiquitin. The basal level of ubiquitin cross-reactivity was detected in the testis and epididymis of control rats (Fig. 3A,B). Both groups (control and treated) showed the accumulation of ubiquitin in the cytoplasmic droplets present in the epididymal spermatozoa (Fig. 3B,C). However, a strong accumulation, suggestive of increased ubiquitin expression and secretion, was detected in the secretory sites (stereocilia and apical blebs) of the epididymal epithelial lining only in the treated rats (Fig. 3D,E). Particularly distinct was the accumulation of ubiquitin in the apical blebs (Hermo & Jacks, 2002), the large bulbous projections of the principal cells through which secretory proteins are released into epididymal lumen (Fig. 3D–F). Using monoclonal antibodies against polyubiquitin chains (MC034), such chains were detected in the testicular stroma and seminiferous tubules of both control (Fig. 4A) and treated (Fig. 4B) rats. Complimentary to the data on increased monoubiquitin secretion in the epididymis of treated rats is the observation that polyubiquitinated substrates accumulated extensively in the clear cells of rat epididymal epithelium (Fig. 4D–F). Clear cells are known for their ability to phagocytose the rejected sperm cytoplasmic droplets and to endocytose disintegrating sperm components and secretory proteins from the epididymal lumen (Hermo et al., 1988). This screening was performed using antibody MC034, which recognizes the isopeptide bond between two ubiquitin molecules, but does not recognize monomeric ubiquitin. It is noteworthy that, whereas the clear cells were present in both control (Fig. 4C) and treated rats, there was an apparent increase in the number of clear cells accumulating polyubiquitin in the epithelium of the treated rats (Fig. 4D). Antibodies against Arylsulfatase A (AsA, green labeling in Figs. 3, 4), a major cellular enzyme responsible for the deglycosylation of sperm plasma membrane glycolipids (Tantibhedhyangkul et al., 2002), revealed the accumulation of this enzyme within the apical blebs containing ubiquitin (Figs. 3D,E, 4D–F). In the epididymis, such expression patterns of AsA complemented ubiquitin expression. Although ubiquitin is capable of causing the degradation of the peptide portion of glycoproteins, the sugar residues of glycoprotein and glycolipid constituents of the sperm plasma membrane would have to be cleaved off by the action of AsA or a similar enzyme, depending on the type of sugar. AsA expression in the epididymis, testis, and in the sperm has been reported previously (Tantibhedhyangkul et al., 2002). Consistent with the degenerative changes seen in the testis of the treated rats, AsA expression there seemed to be reduced (Fig. 4B), compared with control animals (Fig. 4A).

Detection of Apoptosis by a Dual TUNEL–Ubiquitin Assay

A TUNEL assay (Sutovsky et al., 2002) for the detection of single-stranded, apoptotic nuclear DNA was performed on tissue sections in combination with ubiquitin labeling by antibody KM691 (Fig. 5). Neither control (Fig. 5A,B) nor treated rats (Fig. 5E,F) displayed a substantial increase in apoptosis within the seminiferous tubules. A qualitative increase in apoptotic cells was detected in the testicular stroma of the treated rats (Fig. 5E,F). Apoptosis of the stromal Leydig cells could, in part, be responsible for changes in spermatogenesis seen in treated rats by conventional

Figure 4. Polyubiquitin and Arylsulfatase A immunodetection. Detection of polyubiquitin chains by monoclonal antibody MC034, in the testis (**A**, **B**) and epididymis (**C–F**) control (**A**, **C**) and treated (**B**, **D–F**) rats at day 24. Arylsulfatase A (AsA) expression is visualized by green fluorescence. **A:** AsA cross-reactivity around the nuclei of spermatogonia and spermatocytes in the testis of control rats. **B:** A reduced cross-reactivity of AsA (green) and increased polyubiquitin cross-reactivity (red) are seen in the seminiferous tubules and testicular stroma/Leydig cells, respectively, of the treated rats. Note the enlarged lumens of the seminiferous tubules. **C:** Detection of polyubiquitin chains and AsA in the control rat epididymis. **D–F:** A high content of AsA (green) in the apical blebs (arrows) and the accumulation of polyubiquitin (red) in the clear cells (arrowheads) of the treated rat epididymis. Note the increased number of polyubiquitin-containing clear cells in the treated rat (**D**) and their unusual, mushroom-like shape (**F**; arrowheads), probably increasing the endocytosis capability of the apical surface of the epididymal epithelium, facing the lumen of epididymal tubules.

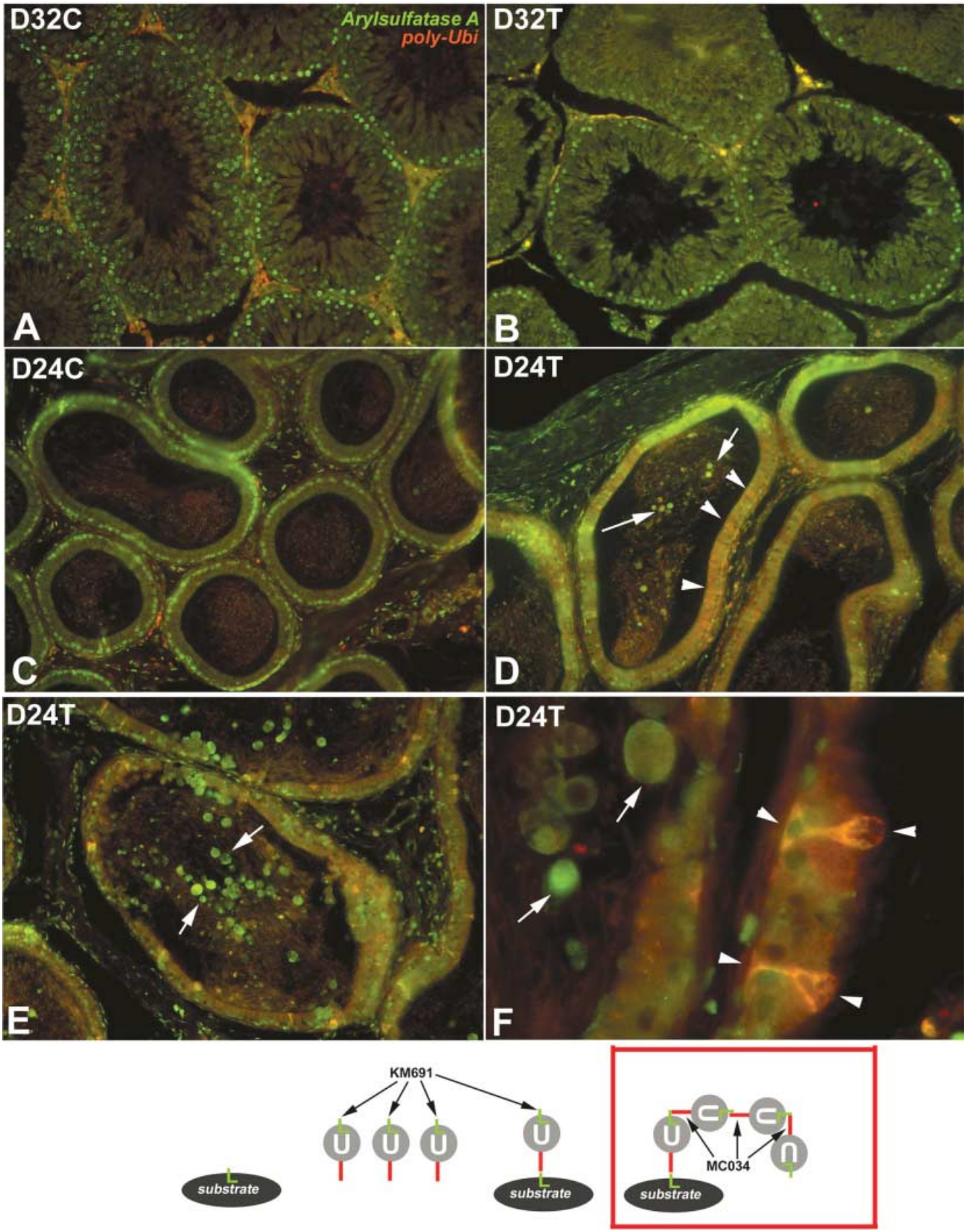

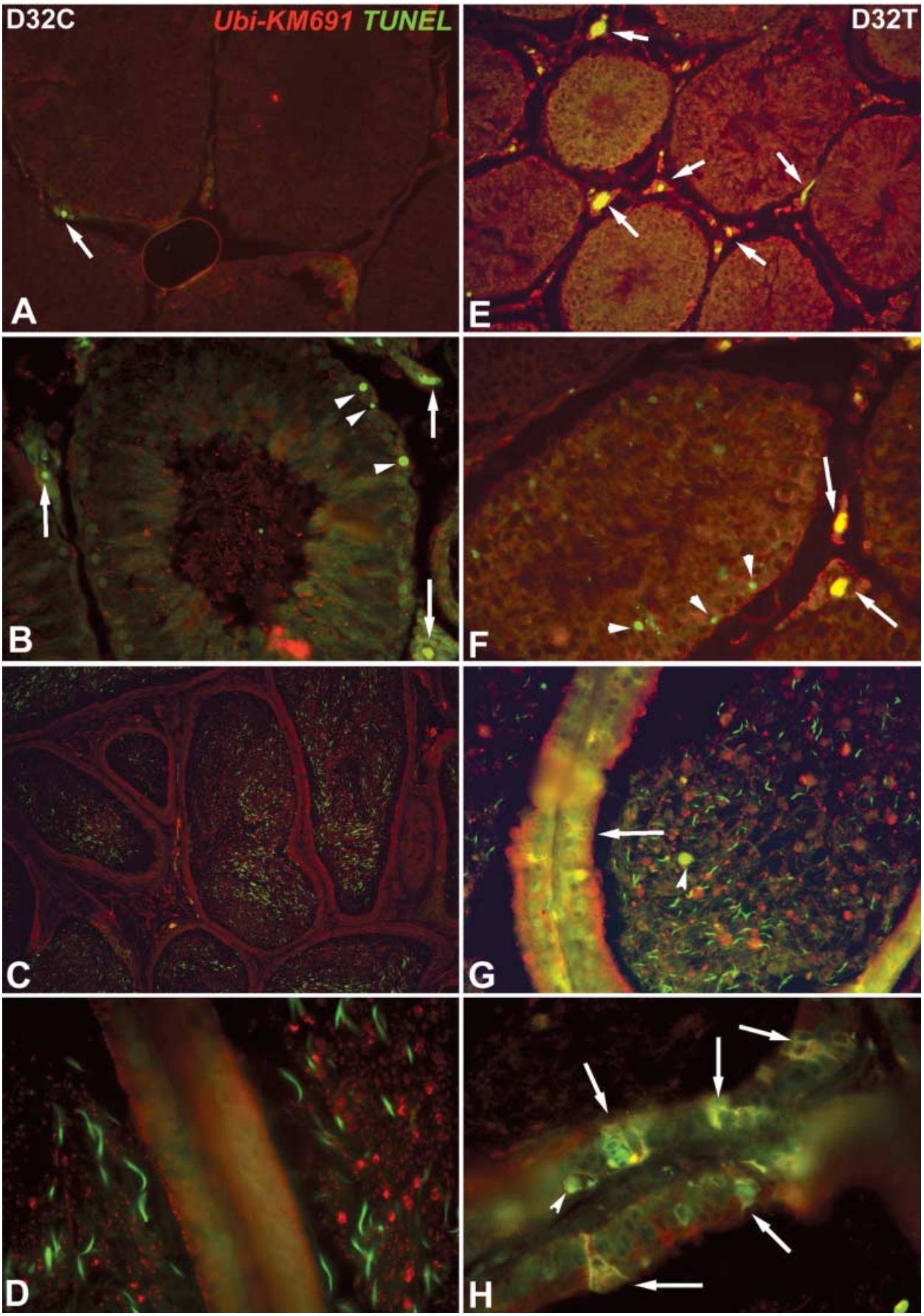

histological analysis. There appeared to be a slight increase in ubiquitin expression within the treated testicular seminiferous tubules (Fig. 5E,F). Similar to the testis, few apoptotic nuclei were detected in the epididymal tissue of control (Fig. 5C,D) and treated rats (Fig. 5G,H). Interestingly, the cytoplasm of the phagocytic clear cells in the treated rats displayed a distinct TUNEL signal (Fig. 5G,H), probably due to the endocytosis of the disintegrated cell nuclei and DNA from the epididymal tubule lumen.

Polyubiquitin Accumulation in the Testis and Epididymis

Tetra- or polyubiquitination is a consensus signal for the degradation of the ubiquitinated proteins by the proteasome, a multisubunit protease/proteolytic organelle (Pickart, 1998). Accordingly, the clear cells of the epididymal epithelium, showing a dramatic increase in polyubiquitin staining after theophylline treatment, also showed a strong signal with antibodies against various α- and β-type proteasomal core subunits (Fig. 6E,F) and β1 (Fig. 6G,H). In control rat epididymis, the abundance and labeling intensity of such clear cells was diminished (Fig. 6A–D). These findings are consistent with the polyubiquitination and proteasomal degradation of the endocytosed, possibly monoubiquitinated proteins from the epididymal lumen.

Discussion

The use of theophylline in the feed for male rats is a well-established model of testicular toxicity, and our findings of decreased organ and testicular weights are consistent with those reported by Morrissey et al. (1988). Our histological findings are also consistent with previous reports (Weinberger et al., 1978; Friedman et al., 1979; personal data). What is new in these data is the progression of changes as imaged with *in vivo* MRM and confirmed with both histology and *ex vivo* MRM (9.4T image data not shown) at an increased resolution. Daston et al. (1987) employed a similar MRI/histology design when studying hydrocephalus in the rat pup. In a similar conclusion, MRI resolution could predict findings confirmed by histology. It is this correlation between noninvasive imaging during a longitudinal experimental design and histology that holds promise for validating the use of numerous imaging technologies in drug safety studies. Noninvasive imaging techniques such as MRM (Dixon et al., 1988) hold several advantages over current methodology and improve toxicological screens by providing proportional information regarding organ volume.

In this longitudinal experimental design, each animal can serve as its control, being imaged prior to the dosing schedule and at reasonable times during dosing. Flexibility can be built in to save a cohort for reversibility, or all dose groups can be processed for rigorous toxicological pathology analysis. Coupling the in-life images with necropsy results, both gross and microscopic, affords the investigator a volumetric and microscopic technique for identifying toxicological findings.

The longitudinal design is especially useful to investigators using rare or valuable animal models (i.e., certain strains of genetically modified mice) or to those limited by the amount of available drug substance, as is commonly seen in initial exploratory toxicology studies of safety and efficacy. *In vivo* MRM does not eliminate the need for toxicological pathology, but it does provide valuable information preceding necropsy, allowing for greater use of information derived from these in-life studies.

One striking feature of the MRM images is the functional information derived from the observation of decreased blood flow in the testis seen in the day-32 group that is accentuated by the presence of gadolinium. Farghali et al. (1991) used the same contrast agent to accentuate changes in testicular blood flow, showing that a decrease in testicular blood flow correlated to an increased change in the testicular image intensity. Our data at 2T indicate that gadolinium is beneficial in imparting contrast to the testis, and that changes in vascular integrity can be semiquantitated by measuring image intensity differences. The pooling of blood or ischemia produced by the decrease in blood flow or breakdown of the blood–testis barrier may be con-

Figure 5. Apoptosis in the rat testis and epididymis. TUNEL assay for the detection of single-stranded, apoptotic nuclear DNA (green), combined with monoubiquitin detection by antibody KM691 (red). Neither the control (**A**, **B**), nor the treated rats (**E**, **F**) displayed a substantial increase in the number of apoptotic cells within the seminiferous tubules (arrow heads), though somewhat more apoptotic cells are present in the testicular stroma of the treated rats (arrows; **E**, **F**). There appeared to be a slight increase in ubiquitin expression within the treated testicular seminiferous tubules (red; **E**, **F**). A few apoptotic nuclei are seen in the epididymal tissue of control (**C**, **D**) and treated rats (arrow heads; **G**, **H**). The cytoplasm of the phagocytic clear cells in the treated rats displays distinct TUNEL signal (arrows; **G**, **H**), possibly due to the endocytosis of the disintegrated cell nuclei removed from lumen the epididymal tubules.

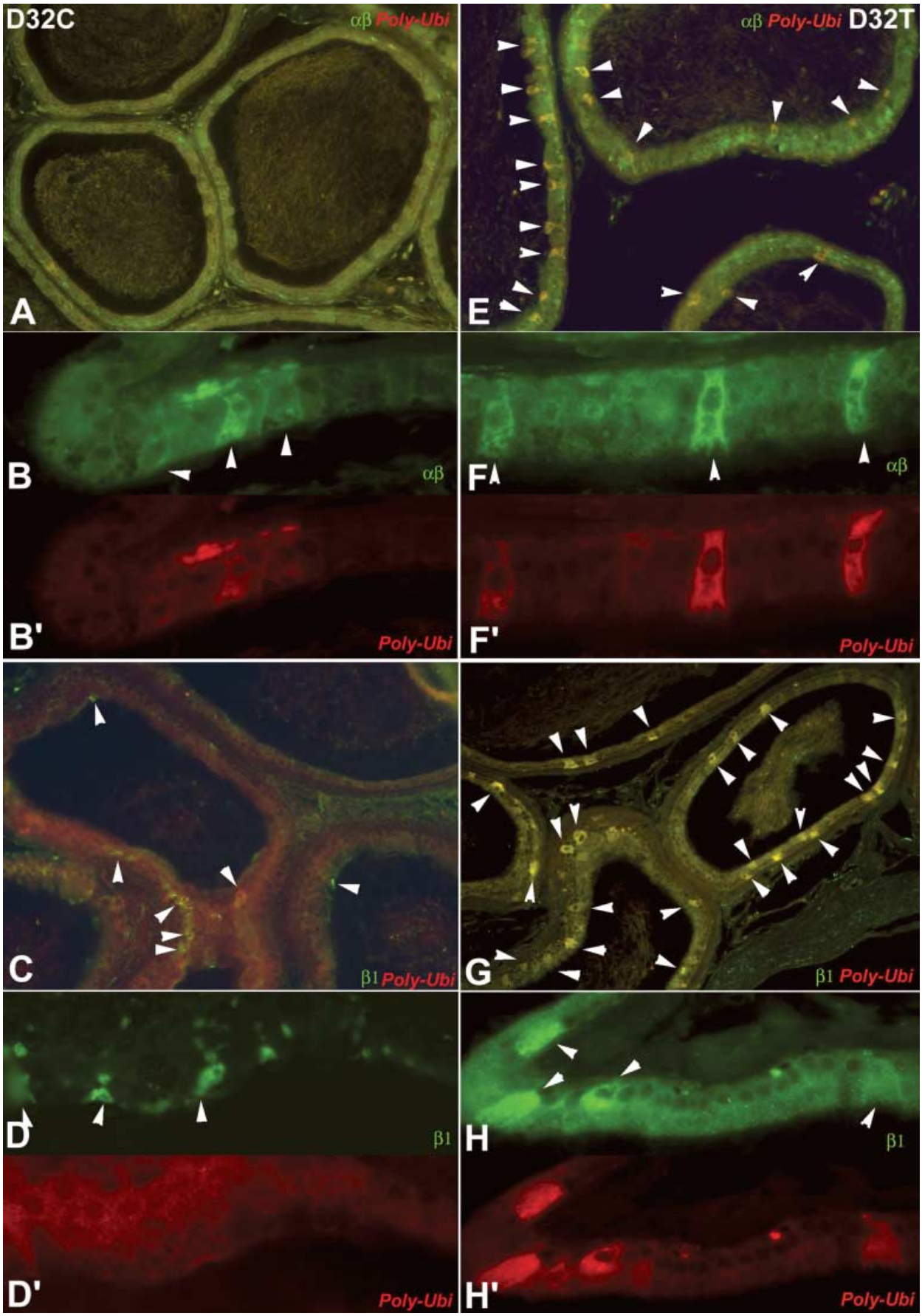

tributory to or a sequel of the overall testis toxicity. The combination of stasis and endothelial leakiness may favor the interaction between gadolinium and free testicular water. This increased interaction is seen by the increase in the T1-weighted signal. The use of gadolinium as an indicator of vascular compromise is best seen in studies of human stroke. The breakdown of the blood–brain barrier allows for penetration into the gray matter, and becomes clearly visible in clinical head scans immediately following the onset of stroke (Maeda et al., 1997). Theophylline does not induce a focal injury, but the change in vascular permeability and leaking of contrast into the tissue is nonetheless observed as an increase in signal intensity at the earliest stage of histopathology (i.e., day 16 of treatment).

The use of MRI in the rat testis as a model for assessing testicular blood flow during spermatic cord torsion and testicular ischemia has been studied and is useful to predict the outcome in clinical instances (Costabile et al., 1993). In this case, an imaging biomarker was useful in predicting likelihood of clinical success. By having a valid animal model for a clinical finding, the process can be broken down and studied. Functional imaging by MRM in our nonclinical species allows for the development of relevant biomarkers for similar human clinical findings. Imaging provides a useful tool for managing risk. Schluter (1989) studied ciprofloxacin toxicity in the dog using MRI, thereby creating a correlative biomarker for juvenile patients receiving this compound. By studying compounds with animal toxicities, it is possible to develop meaningful imaging biomarkers of safety or efficacy, thereby reducing the chance of harm to early human trial participants.

The apparent increase in the number of clear cells accumulating polyubiquitin in the epithelium of the treated rats is furthermore consistent with the increased need for protein/cell removal, endocytosis, and degradation in the epididymis of the treated rats. According to such a scenario, theophylline treatment accelerates the secretion of monoubiquitin by the clear cells in the epididymis. In the epididymal lumen, monoubiquitin binds to proteins and organelles produced by the breakdown of defective spermatozoa and epithelial cells. It is generally accepted that monoubiquitination serves as an endocytotic signal for endocytosis of membrane receptors (Strous & Govers, 1999), though in such case, the monoubiquitination occurs on the cytoplasmic face of cell plasma membrane, and not in the extracellular space or on cell surface. Alternatively, it is possible that the proteins and cellular debris can be polyubiquitinated while still in the epididymal lumen, and the proteasomes could be secreted together with monoubiquitin into epididymal fluid via apical blebs or released from partially degraded spermatozoa. In this scenario, cellular debris from defective spermatozoa could be degraded intraluminally without the need for endocytosis. This could also facilitate the breakdown of damaged spermatozoa and other cells present in the epididymal lumen of theophylline-treated rats. It is thus conceivable that the epididymal fluid creates an environment similar to cell cytosol, complete with the components of the ubiquitin–proteasome proteolytic system and the enzymes necessary for the deglycosylation, ubiquitination, and degradation of sperm proteins and membranes.

MRM as a noninvasive imaging technology is predictive of tissue pathology based on differences in water distribution, and these techniques can be transferred to other toxicology studies. By studying animal models of toxicity, useful biomarkers can be identified for mechanisms of toxicity or safety studies. Additionally, the effects of theophylline treatment specifically on the reproductive system of male rats can be revealed using anti-ubiquitin antibodies, recognizing secretory and endocytic events mediated by the ubiquitin system. It is important to recognize that the expression of the above proteolytic markers, albeit reduced, is also seen in the normal epididymal tissues of untreated rats. Thus, the increased activity of the ubiquitin–proteasome system and related proteolytic activities are likely a part of a physiological response to an increased need for intraluminal degradation of damaged spermatozoa and somatic cells produced by the testis of theophylline-treated rats. The pathology observed in the epididymal epithelium as cell sloughing and apoptosis is further shown to represent removal and destruction of contents from the lumen via an overproduction of proteolytic molecules such as ubiquitin, proteasomal subunits, and Arylsulfatase A. The detection of ubiquitin and proteasomal subunits in the seminal fluid may provide an interesting biomarker for use in toxicology studies. Correlative imaging studies will help advance the development of compounds by managing potential risk to other species, including man.

Figure 6. Ubiquitin subunit staining. Detection of polyubiquitin (red), various α- and β-type proteasomal subunits (green) (**A**, **B**, **E**, **F**) and core subunit β1i (**C**, **D**, **G**, **H**) in the day-32 control (**A–D**) and day-32 treated rat epididymis (**E–H**). The clear cells of the epididymal epithelium (arrowheads) show a dramatic increase in polyubiquitin signal, and a strong signal with antibodies against α/β-types proteasomal subunits (**E**, **F**) and β1 (**G**, **H**), after theophylline treatment. The abundance and labeling intensity of such clear cells is diminished in control rat epididymis (**A–D**). These findings are consistent with the proteasomal degradation of the polyubiquitinated proteins, endocytosed from the epididymal lumen.

Acknowledgments

The authors thank Nat Kopyk for in-life toxicology support, Judy Franco for coordinating animal shipments, Ted Wheeler for animal preparation, Gary Cofer for MRM technical support, and Karen Steever for histologic support. The authors also acknowledge the NIH/NCRR (P41 05959) for funding the CIVM. P.S. was supported by USDA New Investigator Award #99-35203-11743, USDA award #2002-02069, NIH/NIOSH award #7 R21 OH07324-02 and Food for the 21st Century Program of the University of Missouri–Columbia.

References

Callaghan, P.T. (1993). Spatially heterogeneous motion and dynamic NMR microscopy. In *Principles of Nuclear Magnetic Resonance Microscopy*, Callaghan, P.T. (Ed.), pp. 492–501. Oxford, UK: Clarendon Press.

Costabile, R.A., Choyke, P.L., Frank, J.A., Girton, M.E., Diggs, R., Billups, K.L., Moonen, C. & Desjardins, C. (1993). Dynamic enhanced magnetic resonance imaging of testicular perfusion in the rat. *J Urol* **149**, 1195–1197.

Daston, G.P., Neubecker, T.A., Yonker, J.E., Busse, L.J., Pratt, R.G., Samaratunga, R.C. & Thomas, S.R. (1987). Magnetic resonance imaging of congenital hydrocephalus in the rat. *Fundam Appl Toxicol* **9**, 415–422.

Dixon, D., Johnson, G.A., Cofer, G.P., Hedlund, L.W. & Maronpot, R.R. (1988). Magnetic resonance imaging (MRI): A new tool in experimental toxicologic pathology. *Toxicol Pathol* **16**, 386–391.

Farghali, H., Williams, D.S., Gavaler, J. & Van Thiel, D.H. (1991). Effect of short-term ethanol feeding on rat testes as assessed by 31P NMR spectroscopy, 1H NMR imaging, and biochemical methods. *Alcohol Clin Exp Res* **15**, 1018–1023.

Friedman, L., Weinberger, M.A., Farber, T.M., Moreland, F.M., Peters, E.L., Gilmore, C.E. & Khan, M.A. (1979). Testicular atrophy and impaired spermatogenesis in rats fed high levels of the methylxanthines caffeine, theobromine, or theophylline. *J Environ Pathol Toxicol* **2**, 687–706.

Groettrup, M., Kraft, R., Kostka, S., Standera, S., Stohwasser, R. & Kloetzel, P.M. (1996). A third interferon-gamma-induced subunit exchange in the 20S proteasome. *Eur J Immunol* **26**, 863–869.

Hermo, L., Dworkin, J. & Oko, R. (1988). Role of epithelial clear cells of the rat epididymis in the disposal of the contents of cytoplasmic droplets detached from spermatozoa. *Am J Anat* **183**, 107–124.

Hermo, L. & Jacks, D. (2002). Nature's ingenuity: Bypassing the classical secretory route via apocrine secretion. *Mol Reprod Dev* **63**, 394–410.

Hershko, A. (1998). The ubiquitin system: Past, present and future perspectives. In *Ubiquitin and the Biology of the Cell*, Peters, J.-M., Harris, J.R. & Finley, D. (Eds.), pp. 1–17. New York: Plenum Press.

Hochstrasser, M. (2002). Molecular biology. New proteases in a ubiquitin stew. *Science* **298**, 549–552.

Lauterbur, P.C. (1973). Image formation by induced local interactions: Examples employing nuclear magnetic resonance. *Nature* **242**, 190–191.

Lippert, T.H., Seeger, H., Schieferstein, G. & Voelter, W. (1993). Immunoreactive ubiquitin in human seminal plasma. *J Androl* **14**, 130–131.

Maeda, M., Maley, J.E., Crosby, D.L., Quets, J.P., Zhu, M.W., Lee, G.J., Lawler, G.J., Ueda, T., Bendixen, B.H. & Yuh, W.T. (1997). Application of contrast agents in the evaluation of stroke: Conventional MR and echo-planar MR imaging. *J Magn Reson Imaging* **7**, 23–28.

Morrissey, R.E., Collins, J.J., Lamb, J.C., Manus, A.G. & Gulati, D.K. (1988). Reproductive effects of theophylline in mice and rats. *Fundam Appl Toxicol* **10**, 525–536.

Pickart, C.M. (1998). Polyubiquitin chains. In *Ubiquitin and the Biology of the Cell*, Peters, J.-M., Harris, J.R. & Finley, D. (Eds.), pp. 19–63. New York: Plenum Press.

Santamaria, L., Martin, R., Paniagua, R., Fraile, B., Nistal, M., Terenghi, G. & Polak, J.M. (1993). Protein gene product 9.5 and ubiquitin immunoreactivities in rat epididymis epithelium. *Histochemistry* **100**, 131–138.

Schluter, G. (1989). Ciprofloxacin: Toxicologic evaluation of additional safety data. *Am J Med* **87**, 37S–39S.

Strous, G.J. & Govers, R. (1999). The ubiquitin-proteasome system and endocytosis. *J Cell Sci* **112**, 1417–1423.

Sutovsky, P., Moreno, R., Ramalho-Santos, J., Dominko, T., Thompson, W.E. & Schatten, G. (2001*a*). A putative, ubiquitin-dependent mechanism for the recognition and elimination of defective spermatozoa in the mammalian epididymis. *J Cell Sci* **114**, 9–75.

Sutovsky, P., Neuber, E. & Schatten, G. (2002). Ubiquitin-dependent sperm quality control mechanism recognizes spermatozoa with DNA defects as revealed by dual ubiquitin-TUNEL assay. *Mol Reprod Dev* **61**, 406–413.

Sutovsky, P., Terada, Y. & Schatten, G. (2001*b*). Ubiquitin-based sperm assay for the diagnosis of male factor infertility. *Hum Reprod* **16**, 250–258.

Tanaka, K. & Tsurumi, C. (1997). The 26S proteasome: Subunits and functions. *Mol Biol Rep* **24**, 3–11.

Tantibhedhyangkul, J., Weerachatyanukul, W., Carmona, E., Xu, H., Anupriwan, A., Michaud, D. & Tanphaichitr, N. (2002). Role of sperm surface Arylsulfatase A in mouse spermzona pellucida binding. *Biol Reprod* **67**, 212–219.

Thompson, W.E., Sutovsky, M., Fischer, K.A., Safranski, T., Moreno, R., Ramalho-Santos, J. & Sutovsky, P. (2002). Differential ubiquitination of prohibitin, p64/lillie and tubulin in mammalian spermatozoa isolated from testis, epididymis and ejaculate (Abstract). *Biol Reprod* **66**, 161.

Wehrli, F.W., Shaw, D. & Kneeland, J.B. (1988). *Biomedical Magnetic Resonance Imaging*. New York: VCH Publishers.

Weinberger, M.A., Friedman, L., Farber, T.M., Moreland, F.M., Peters, E.L., Gilmore, C.E. & Khan, M.A. (1978). Testicular atrophy and impaired spermatogenesis in rats fed high levels of the methylxanthines caffeine, theobromine, or theophylline. *J Environ Pathol Toxicol* **1**, 669–688.